DOI: 10.1002/chem.200601154

Synthesis and Structure–Property Relationships of Amphiphilic Organogelators

Nils Mohmeyer and Hans-Werner Schmidt*[a]

Abstract: A series of low-molecular-weight amphiphilic molecules was synthesized and investigated for their ability to gel organic solvents. These amphiphilic molecules are composed of a head-group moiety capable of forming intermolecular associations through hydrogen bonds and *n*-alkyl chains of various lengths. This paper describes the continuation of recently published work, in which this class of gelators was presented for the first time. Here, the focus addresses systematically three different structural variations of the head-group moiety: 1) the rigidity, 2) the type and strength of the hydrogen-bond-forming units, and 3) the reduction of the intermolecular interaction by incorporating a lateral substituent. The gelation behavior was investigated in *p*-xylene and in several polar solvents. The aim was to establish structure–property relationships and to provide organogelators capable of forming gels at low concentrations with adjustable sol–gel transition temperatures and good optical quality. For some individual compounds of the series this property profile was achieved. For the investigated solvents, with particular compounds, sol–gel transition temperatures above 100 °C with a reasonable concentration of gelator are obtainable.

Keywords: amphiphiles · gels · self-assembly · sol–gel processes · supramolecular chemistry

Introduction

Organogelators are low-molecular-weight organic molecules that are capable of growing from homogeneous solution into fine fibrillar dendritic structures within the organic solvent. These fibrillar structures build a continuous three-dimensional network resulting in a macroscopic gel formation. The field of organogelators has attracted interest due to industrial applications in many areas such as cosmetics, polymers, and soft condensed matter with advanced functions.[1–16] The process of these self-assembly-type gelators is driven by specific noncovalent intermolecular interactions. The physical gels formed are therefore thermoreversible. By heating above the sol–gel transition temperature the gelator is completely dissolved and upon cooling to room temperature, the three-dimensional network and thus the gel will be obtained. The intermolecular interactions are typically generated by electrostatic interactions, π–π stacking, metal-coordination-bond formation, dipole–dipole interactions, and/or hydrogen bonds. Intensive effort has been expended to understand the structure–property relationships to tailor organogelators; however, until now it has not been possible to predict in advance if a new molecule will gel an organic solvent or not. Therefore, in recent years, many researchers have attempted to find new efficient gelators, resulting in the discovery of a variety of small molecules. A selection of some representatives includes 1,3:2,4-di-*O*-benzylidene-D-sorbitol (DBS),[17–19] 2,3-bis-*n*-decyloxyanthracene,[20,21] cholesterol derivatives,[22–24] fluorinated or bolaform amides,[25,26] symmetrical dialkylamides,[27] symmetrical mono- and bisureas,[8,28–30] nonsymmetrical bisureas,[31] and *N*-*n*-octyl-D-gluconamide.[32,33] Recently, we added to this selection a class of amphiphilic molecules consisting of a head moiety capable of forming intermolecular hydrogen bonds and a hydrophobic long alkyl chain.[34] In more detail, the investigated molecules consist of three different structural units: an apolar terminal cyclohexyl group, a hydrogen-bond-forming segment based on *p*-phenylenediamines with amide and urea groups, and a long alkyl chain with more than eight carbon atoms. The *para* linkage used provides the rigidity of the head-group moiety.[34]

Continuing from this work, we now expand the class of amphiphilic gelators by different structural variations of the head-group moiety. With this intention, the rigidity of the

[a] Dr. N. Mohmeyer, Prof. Dr. H.-W. Schmidt
Macromolecular Chemistry I
Bayreuther Institut für Makromolekülforschung (BIMF) and
Bayreuther Zentrum für Grenzflächen und Kolloide (BZKG)
University Bayreuth, 95440 Bayreuth (Germany)
Fax: (+49) 921-55-3206
E-mail: hans-werner.schmidt@uni-bayreuth.de

head group will be reduced by a *meta* substitution (i). The type and strength of the hydrogen-bond-forming units will be varied (ii) and finally, the intermolecular interaction will also be reduced by the use of a lateral substituent R (iii). Furthermore, combinations of these approaches will be investigated.

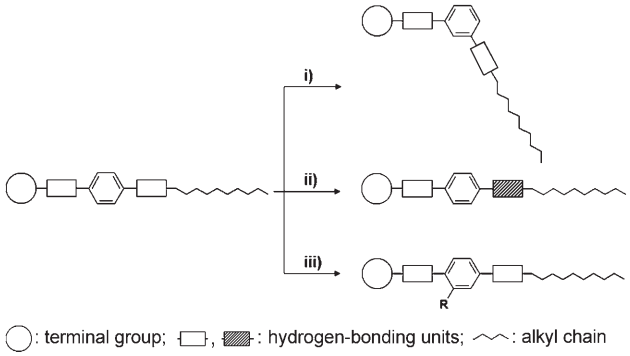

The aim is to investigate the influence of these structural variations and by this, to establish structure–property relationships with respect to the formation of gels, to adjust sol–gel transition temperatures and mechanical strength, and to improve the optical quality, all at the lowest possible gelator concentration. We focused on the apolar solvent *p*-xylene and on polar solvents such as γ-butyrolactone, valeronitrile, and especially 3-methoxypropionitrile with respect to their application possibilities in dye-sensitized solar cells.[5,19,35,36]

Results and Discussion

Synthesis: The synthetic route to the eight different series (each with three compounds) of amphiphilic bisamides and amide-/urea-functionalized derivatives is shown in Scheme 1. In the first step, cyclohexanecarboxylic acid chloride was allowed to react with the four different nitro-group-containing aromatic amines **1a–d** in dry *N*-methyl-2-pyrrolidone (NMP) and pyridine. These amines were selected to introduce different structural variations in the head-group moiety. 4-Nitroaniline **1a** was selected to obtain a linear and rigid moiety and 3-nitroaniline **1b** to introduce a kink within the head group. Two other nitroaniline derivatives **1c–d** were chosen to reduce the intermolecular interactions by a lateral methyl substituent. The four resulting nitro compounds were reduced in the second step with hydrogen, by using palladium on activated carbon as catalyst, to the corresponding amine derivatives **2a–d**. These four amines were reacted with octanoyl chloride, tetradecanoyl chloride, and octadecanoyl chloride to obtain the *para*-bisamides **3a–c**, the *meta*-bisamides **4a–c**, and the methyl-substituted derivatives **5a–c** (*para*) and **6a–c** (*meta*). To introduce a urea group instead of the second amide group, the amino compounds **2a–d** were reacted with isocyanates of different chain lengths (-C_8, -C_{14}, and -C_{18}) to obtain the *para*-substituted amide-/urea-functionalized derivatives **7a–c**, the *meta*-substituted derivatives **8a–c**, and also the methyl-functionalized derivatives **9a–c** (*para*) and **10a–c** (*meta*).

Structure–property relationships with respect to gelation ability: In general, gelation ability, efficiency, and gel properties change dramatically with small structural variations in the gelator molecule and depend also on the solvent used. The gelation ability was investigated in *p*-xylene as apolar hydrocarbon and in valeronitrile, γ-butyrolactone, and 3-methoxypropionitrile as polar solvents. The latter are of special interest due to their potential application in quasi-solid-state dye-sensitized solar cells.[36]

To efficiently screen the principle gelation ability, mixtures of these compounds at 1 wt% in the given solvents were heated until the solid was, if possible, completely dissolved. The homogenous solutions were cooled slowly to room temperature and gelation was observed visually. Gelation was considered to have occurred when a gel state that exhibited no gravitational flow over a period of several hours was obtained. This process was repeated several times, demonstrating the thermoreversibility of the gelation and dissolution process.

For a better understanding of the structure–property relationships, Figure 1 illustrates the marginal chemical modifications of the compounds conducted and Table 1 summarizes the results of the screening experiments. The following discussion begins with the series of *para*-substituted rigid bisamides **3a–c**[34] and is structured in comparative sets consisting in each case of two series of three compounds. Firstly, the reduction of the rigidity of the head-group moiety is discussed. The modification from the rigid *para*-bisamides **3a–c** to the kinked *meta*-bisamides **4a–c** changes the gelation ability dramatically. The *para*-substituted bisamides **3a–c** gel *p*-xylene with a minimum required gelator concentration of between 1.1 and 1.5 wt%. All *meta*-bisamides **4a–c** are soluble in *p*-xylene at elevated temperatures, precipitate upon cooling, and do not form gels. In the polar solvents, valeronitrile, γ-butyrolactone, and 3-methoxypropionitrile, all *para*-bisamides **3a–c** precipitate with one exception. Compound **3c** is able to gel γ-butyrolactone at an interestingly low concentration of only 0.5 wt%. In contrast to this, most of the *meta*-bisamides **4a–c** are highly soluble and stay in solution. The second variation is the replacement of the amide group next to the alkyl chain by a urea group yielding the amide-/urea-functionalized derivatives **7a–c**.[34] All three compounds gel *p*-xylene at a much lower required gelator concentration relative to **3a–c**. A remarkable improvement of the gelation ability was observed for the polar solvents. Here, compounds **7b** and **7c** gel all selected polar solvents at a very low concentration. The introduction of a lateral methyl substituent on the aromatic ring in the 2-position next to the amide group also has slight influence on the gelation ability. In comparison to the bisamides **3a–c**, the molecules **5b** and **5c** gel *p*-xylene at concentrations of below 0.5 wt%. This variation is the most interesting one due to the immense influence on the thermal and optical properties

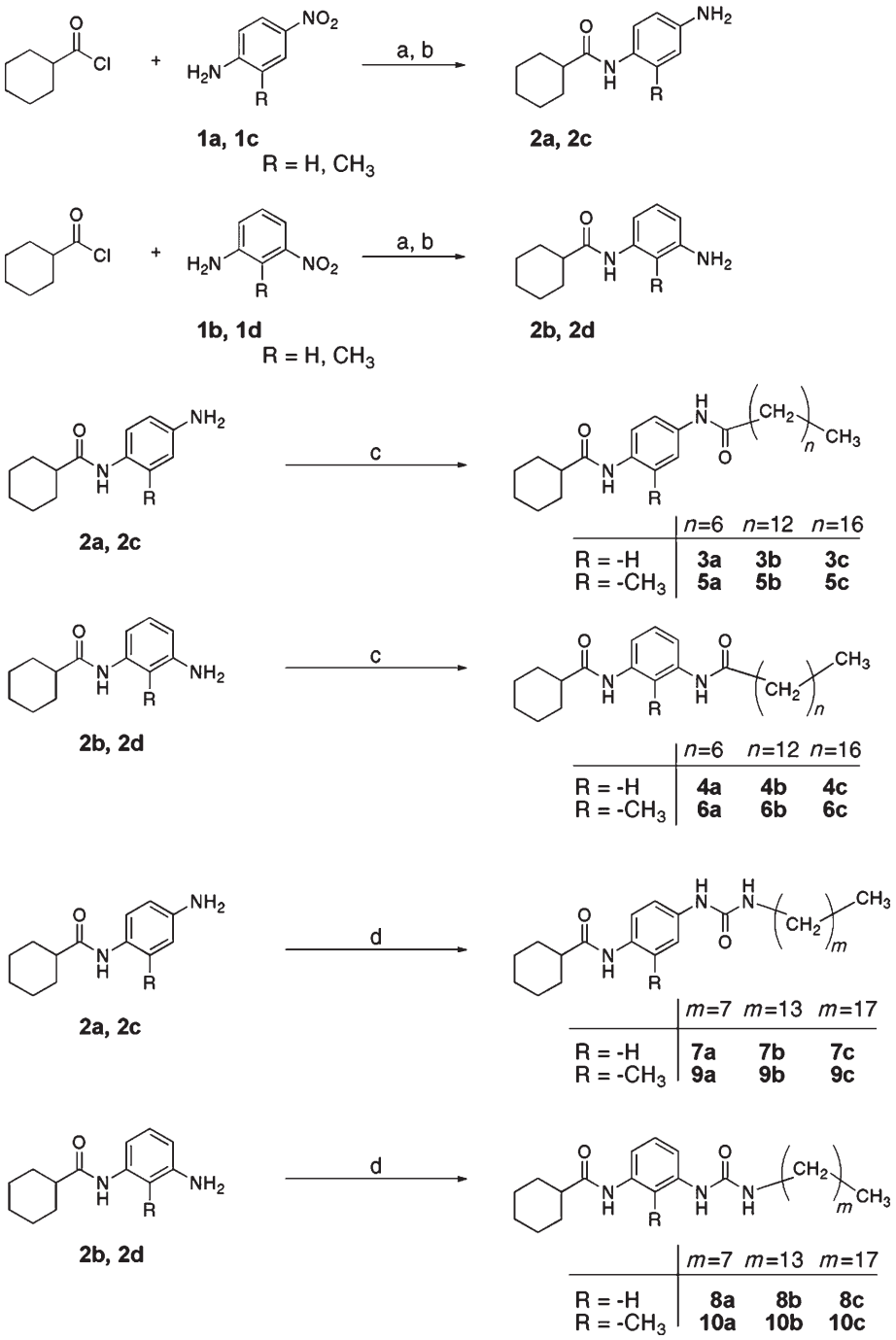

Scheme 1. Synthesis of the asymmetrically substituted phenylenediamine-based bisamide derivatives **3a–c**, **4a–c**, **5a–c**, and **6a–c** and the amide-/urea-functionalized derivatives **7a–c**, **8a–c**, **9a–c**, and **10a–c**. a) NMP, pyridine, 80 °C, 2 h; b) Pd/C, H_2, THF/MeOH, 3.5 bar, 40 °C, 24 h; c) aliphatic acid chloride, NMP, pyridine, 80 °C, 2 h; d) aliphatic isocyanate, THF, reflux, 2 h.

of the gel systems, which will be discussed later. The derivatives **5b** and **5c** are also able to gel valeronitrile at concentrations of 0.5 and 0.75 wt %, respectively.

In this section, the structural modification from a rigid to a kinked head-group moiety will be discussed. As mentioned above, from compounds **3a–c** to **4a–c**, the gelation ability decreases. The same trend was observed for the series of the amide-/urea-functionalized derivatives **7a–c** versus **8a–c**. The rigid derivatives **7b** and **7c** show good gelation ability in all four solvents investigated, whereas the kinked derivatives **8b** and **8c** precipitate upon cooling. Comparison of the amide-/urea-functionalized derivatives **9a–c** and **10a–c** reveals that the gelation ability decreases by introduction of the kink. The compounds **10a–c** are in most cases insoluble or precipitate. The difference in the gelation ability of the methyl-substituted derivatives **5a–c** and **6a–c** is only marginal. In apolar solvents the kinked derivatives **6a–c** exhibit the better gelation behavior; however, in polar solvents the rigid derivatives are more efficient.

With respect to the next structural variation—the replacement of one amide group by a urea group—the gelation ability changes non-uniformly within the four comparative sets. Within the two sets of the rigid head-group moieties the gelation capability is increased from both bisamide series **3a–c** and **5a–c** to the amide-/urea-functionalized derivatives **7a–c** and **9a–c**. However, the kinked bisamides **4a–c** and **6a–c** compared to the kinked amide-/urea-functionalized derivatives **8a–c** and **10a–c** show only slight changes with no clear tendency.

The introduction of the lateral methyl substituent improves the gelation behavior within the two comparative sets with kinked head-group moieties. Compared to the series **4a–c** and **8a–c** without methyl substituents, the methyl-substituted derivatives **6a–c** and **10a–c** exhibit an enhanced tendency to form gels. Within the sets of compounds with rigid head groups the gelation ability is qualitatively similar.

All these results support that a well-balanced system of rigidity, intermolecular interactions driven by amide or urea units, and a slight packing disruption by the lateral methyl substituent can be balanced to obtain gels at low gelator

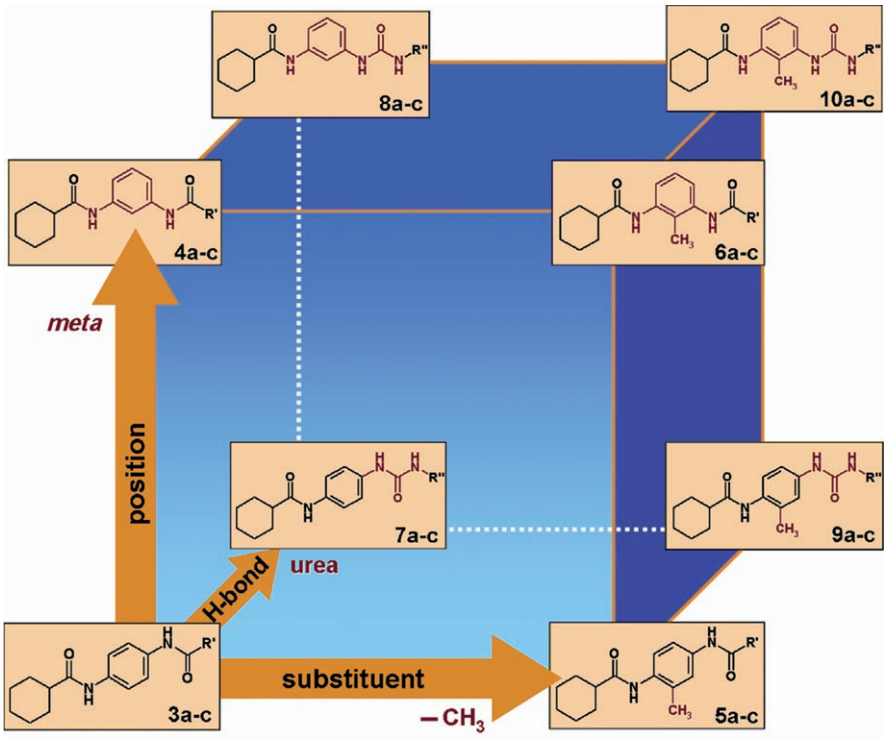

Figure 1. Schematic representation of synthesized amphiphilic compounds ordered by their structural variation. Starting series: **3a–c**. Change in *x* axis direction: introduction of a lateral methyl group at the head-group moiety; change in *y* axis direction: reduction of rigidity by introducing a kink due to *meta* linkage at the head-group moiety; change in *z* axis direction: variation in the type and strength of the intermolecular interactions by replacing an amide group by a urea group.

Table 1. Comparison of gelation abilities of the synthesized amphiphilic compounds in different solvents at a concentration of 1 wt%. For gel formation at room temperature, the minimum required concentration in wt% is given in parentheses; gel: formation of stable gel; insol.: compound is not completely soluble at the boiling temperature of the solvent; ppt.: compound precipitates upon cooling; sol.: compound stays in solution after cooling.

Compound	*p*-Xylene	Valeronitrile	γ-Butyrolactone	3-Methoxypropionitrile
3a	gel (1.1)	ppt.	ppt.	ppt.
3b	gel (1.5)	ppt.	ppt.	ppt.
3c	gel (1.5)	ppt.	gel (0.5)	ppt.
4a	ppt.	sol.	sol.	sol.
4b	ppt.	sol.	sol.	ppt.
4c	ppt.	sol.	ppt.	ppt.
5a	ppt.	ppt.	ppt.	ppt.
5b	gel (0.5)	gel (0.5)	gel (1.0)	ppt.
5c	gel (0.25)	gel (0.75)	ppt.	ppt.
6a	gel (0.25)	ppt.	ppt.	ppt.
6b	gel (0.25)	gel (2.0)	ppt.	ppt.
6c	gel (0.5)	ppt.	ppt.	ppt.
7a	gel (0.3)	gel (0.5)	ppt.	ppt.
7b	gel (0.25)	gel (0.25)	gel (1.0)	gel (0.25)
7c	gel (0.2)	gel (0.05)	gel (0.75)	gel (0.25)
8a	ppt.	sol.	sol.	sol.
8b	ppt.	ppt.	ppt.	ppt.
8c	ppt.	ppt.	ppt.	ppt.
9a	insol.	gel (0.25)	gel (0.75)	gel (0.75)
9b	gel (0.25)	gel (0.75)	gel (1.0)	gel (0.5)
9c	gel (0.25)	gel (1.5)	ppt.	gel (0.75)
10a	insol.	insol.	ppt.	insol.
10b	insol.	gel (1.5)	ppt.	ppt.
10c	gel (0.25)	gel (0.5)	ppt.	ppt.

concentration. In general within this systematic study, the change from the rigid to the kinked compounds does not improve the gelation ability. More-favorable structural changes are the replacement of one amide group by a urea group and the introduction of a lateral methyl substituent. Finally, the variation in the length of the alkyl chain shows a minor effect relative to the other variations reported here. Following these more-qualitative investigations, the next section discusses the concentration dependence on selected compounds.

Gel properties as a function of concentration: *p*-xylene

In this section, the gelation properties in *p*-xylene are discussed in particular as a function of the gelator concentration. For selected compounds, the thermal and optical properties are presented.

Sol–gel transition temperature: An important property of organogelators is the sol–gel transition temperature (T_{gel}). This thermoreversible transition depends mainly on the concentration of the gelator and the type of solvent used. The sol–gel transition temperature defines the application range and processing temperature of organogels. T_{gel} was determined by the dropping-ball method.[30]

As generally observed, the sol–gel transition temperature decreases as the gelator concentration decreases. However, the concentration range in which the organogelator forms stable gels differs as the chemical structure and type of organic solvent varies. Above a certain concentration, the gelator is not completely soluble. This is also limited by the boiling point of the solvent. Below a certain

concentration, the concentration is too low to form a three-dimensional network. Only a viscosity increase is observed. Figure 2 displays the influence of the gelator concentration on the sol–gel transition temperatures within the concentration range of 0.25 to 3.0 wt%. Figure 2, top, compares the influence of the type of hydrogen-bonding units in the head-group moiety (bisamide or amide/urea). Bisamide **5b** exhibits its sol–gel transition temperatures from 86 to 102 °C within the concentration range of 0.5 to 2.5 wt%. Below 0.5 wt% **5b** is not able to from a stable gel, whereas above 2.5 wt% the compound is not completely soluble in boiling *p*-xylene. In contrast, the sol–gel transition temperatures with the corresponding amide-/urea-functionalized derivative **9b** are about 20–30 °C higher. This increase was also observed in the comparison of **6c** and the amide-/urea-functionalized derivatives **10c**. However, **10c** shows lower solubility in boiling *p*-xylene than the three other compounds. Compound **10c** is only completely soluble up to a concentration of 1.0 wt% with a T_{gel} of 137 °C, which is 40 °C higher than that of the corresponding bisamide **6c**. This solubility is limited by the boiling point of *p*-xylene at 138 °C. The general tendency that *p*-xylene gels with the amide-/urea-functionalized derivatives (**9b** and **10c**) show higher T_{gel} values than the corresponding bisamides (**5b** and **6c**) is attributed to an additional hydrogen bond formed by the second nitrogen at the urea group in contrast to the amide group.

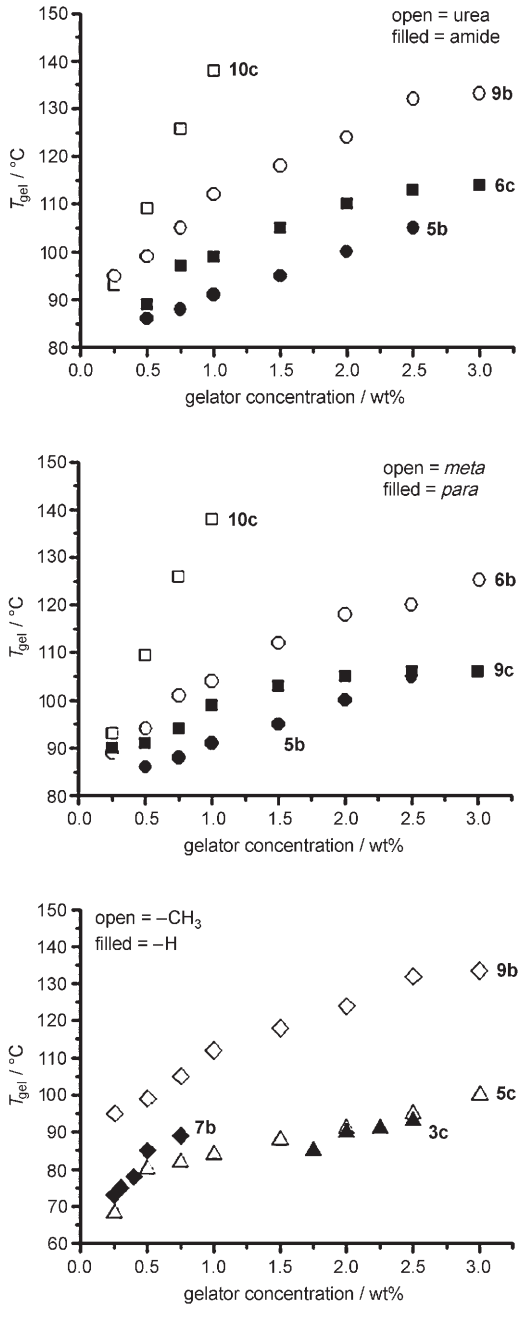

Figure 2. Sol–gel transition temperature as a function of the gelator concentration of several compounds in *p*-xylene. The influence of the different structural variations of the compounds is illustrated. Top: comparison of hydrogen-bonding units (amide or urea); middle: comparison of the position at the aromatic ring (*para* or *meta*); bottom: comparison of the substitution in the 2-position (with or without methyl group).

Figure 2, middle, shows the influence of structural modification from a rigid to a kinked head-group moiety on T_{gel}. This will also be discussed by means of four compounds, all with a lateral methyl substituent. The gelation behavior of compound **5b** with the rigid head-group moiety was discussed above and features only moderate T_{gel} values. In comparison, the corresponding derivative **6b** with the kinked head-group moiety induces, at concentrations of between 0.5 and 2.5 wt%, T_{gel} values 10–20 °C higher than those for compound **5b**. This result was also observed in the comparison of derivatives **9c** and **10c**, although it was not expected. From the geometrical point of view, the intermolecular interactions of the *para*-linked rigid derivatives **5b** and **9c** should be stronger than the ones for the kinked, flexible *meta*-linked compounds **6b** and **10c**. In *para*-linked head-group moieties the molecular packing should be easier and the intermolecular interactions stronger, leading to more-stable supramolecular aggregates. However, the contrary was the case.

In the case of the introduction of the lateral methyl substituent (Figure 2, bottom), an unexpected behavior was also observed. The two bisamides **3c** and **5c** show nearly the same T_{gel} values. However, compound **5c** forms stable gels over the entire concentration range investigated, whereas compound **3c** forms stable gels only within a limited concentration range of between 1.75 and 2.5 wt%. Below this concentration, only highly viscous solutions were obtained and above 2.5 wt%, the compound is not completely soluble. The same trend was observed with the amide-/urea-functionalized derivatives **7b** and **9b**. Here too, the derivative with the lateral methyl substituent forms gels over the entire concentration range. In addition, the sol–gel transition temperature of **9b** is substantially higher than that of **7b**. For example, at a concentration of 0.5 wt%, compound **7b** exhibits a sol–gel transition temperature of 85 °C, whereas the T_{gel} value for compound **9b** is 99 °C.

Details of the intermolecular interaction can be investigated by FTIR spectroscopy. The characteristic IR vibrations of amide and urea groups are the C–N stretching,

N–H stretching and bending vibration, and more importantly, the C=O stretching vibration. These vibrations appear at different wavenumbers for free or hydrogen-bonded amide and urea groups, respectively. In addition, the strength of the hydrogen bonds shifts the location of the vibrations in the spectra. The amide I (C=O stretching) and amide II (C–N stretching and N–H bending) vibrations are located between 1500 and 1700 cm^{-1}. In this discussion we focus on the shift of the C=O stretching vibration. For amide groups, free C=O stretching vibrations are located at around 1685 cm^{-1}, whereas associated hydrogen-bonded C=O stretching vibrations are located at around 1660 cm^{-1}.[37] In the case of urea groups, the free C=O stretching vibration is located between 1680 and 1690 cm^{-1}, and the associated hydrogen-bonded C=O stretching vibration is located between 1630 and 1655 cm^{-1}.[38,39]

Figure 3 shows FTIR spectra of *p*-xylene gels with derivative **9b** (top) with the lateral methyl substituent in the head-group moiety, and the corresponding derivative **7b** (bottom) without methyl substituent, at three different concentrations (0.25, 0.5, and 0.75 wt%). The IR spectra of the gels with compound **9b** for different concentrations showed two signals with the same proportion. The signal at 1630 cm^{-1} is caused by the C=O stretching vibration of the urea group in its hydrogen-bridged form. The second signal at 1652 cm^{-1} corresponds to the amide group, also in its associated form. The spectra of gels with compound **7b** appear different. The strongest signal is at 1635 cm^{-1} and is, as in the case above, also related to the hydrogen-bonded C=O stretching vibration of hydrogen-bonded urea groups. A clear difference was observed for the amide groups. The spectra show a signal at 1681 cm^{-1}, which we allocate to the presence of free nonassociated amide groups. This is further supported by the missing C=O stretching vibration of associated amide groups, which are barely visible at about 1655 cm^{-1}. This confirms that the organogelator **9b** has a better packing and stronger intermolecular interaction of the head-group moiety, despite the lateral methyl substituent. This means a twist of the phenyl out of the amide/urea planes with less hindrance. As the hydrogen bonding is apparent, it is reasonable to suggest that a conformational effect that enforces hydrogen bonding in the case of the compound with the additional methyl group **9b** is operating. Consequently, the sol–gel transition temperatures are, relative to compound **7b**, higher (Figure 2, bottom).

Optical and morphological properties: For applications, the optical properties of organogels are of special interest. The goal is the preparation of transparent gels with excellent clarity and haze. These properties are thickness dependent and can be measured by using standardized equipment.[40] Most sensitive is the haze value, which is attributed to scattering above an angle larger than 2.5°. The haze value varies from 100% for a highly scattering opaque material to 0% for a clear liquid, such as water. For the measurements, a homogeneous solution of the gelator in *p*-xylene at elevated temperatures was carefully filled in a disc-shaped quartz cell with a diameter of 18 mm and a thickness of 10 mm. After cooling to room temperature at a cooling rate of 5 °C min^{-1}, the gels were maintained at room temperature for 24 h before performing the measurement. Figure 4 shows

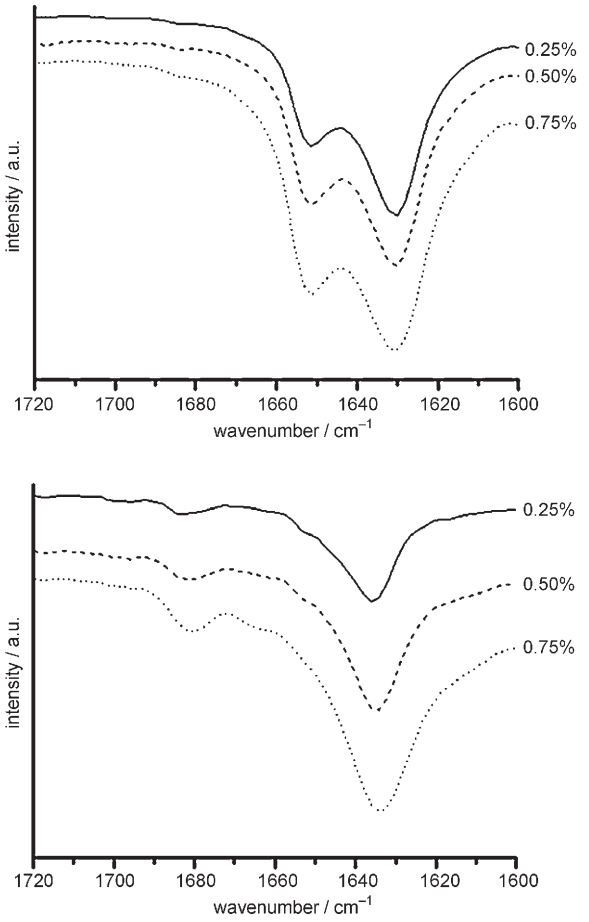

Figure 3. Sections of the IR spectra of *p*-xylene gels comprising different concentrations of **9b** (top) and **7b** (bottom) measured at room temperature showing the differences in the amide I vibration.

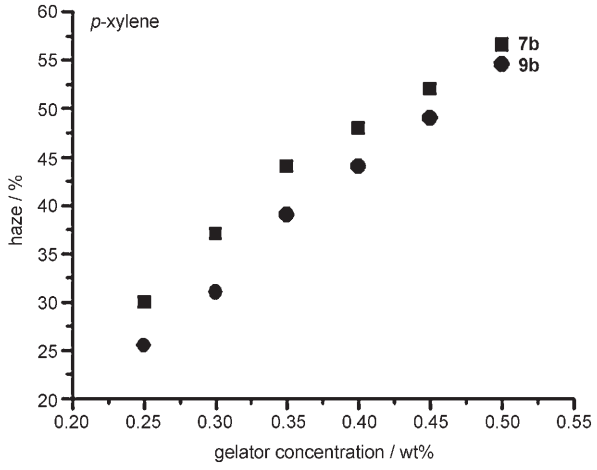

Figure 4. Optical properties of *p*-xylene gels comprising different concentrations of **7b** (■) and **9b** (●). The haze values were measured by using a disc-shaped quartz cell with a thickness of 10 mm.

the haze values of the *p*-xylene gels for compounds **7b** and **9b** as a function of the concentration. At all concentrations, the haze values of the *p*-xylene gels comprising the derivative **9b** are lower than for derivative **7b**. In both cases the haze values increase as gelator concentration increases, most probably due to an increase in size of the fibrillar nanostructures. The best haze value of 25% was observed with compound **9b** at a concentration of 0.25 wt%. At the same concentration, **7b** had a haze value of 30%.

To understand the difference in the optical properties between the *p*-xylene gels, transmission electron microscopy (TEM) and scanning electron microscopy (SEM) were carried out. The samples for TEM were prepared by forming the gel on a grid and slowly evaporating the solvent at room temperature under vacuum. Figure 5, top and middle, display the TEM images of the three-dimensional-network structures formed from a 0.5-wt% gel of compounds **7b** and **9b**. The amide-/urea-functionalized derivative **7b** without the methyl substituent forms long fibrils with diameters of between 100 and 200 nm. In comparison, the TEM image of the network system of compound **9b** with the lateral methyl substituent reveals thinner and more-uniform fibrillar structures with an average thickness of about 50 nm. This observation is in agreement with the results of the optical measurements, in which the gels based on compound **9b** exhibit lower haze values. The three-dimensional-network structure can also be visualized by SEM after removal of the *p*-xylene with supercritical carbon dioxide (sc-CO_2). Figure 5, bottom, shows the network structure of **9b** for a sample prepared from a gel with a gelator concentration of 1.0 wt%.

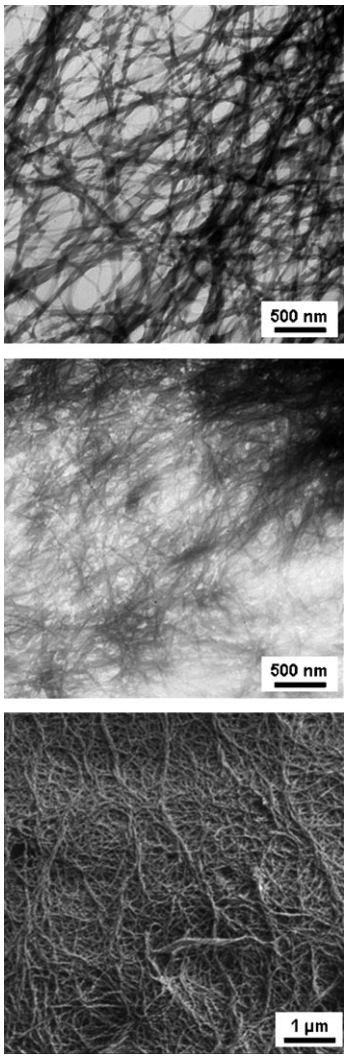

Figure 5. Electron microscopy images of network structures. Top: TEM image of **7b** after evaporation of *p*-xylene (initial gelator concentration: 0.5 wt%); middle: TEM image of **9b** (0.5 wt%) after evaporation of *p*-xylene; bottom: SEM image of **9b** (1 wt%) after removal of *p*-xylene with sc-CO_2.

Gel properties as function of concentration: polar solvents

In this section we briefly review the gelation capability in the two polar solvents, valeronitrile and 3-methoxypropionitrile. For this, the best candidates, the two bisamides **5b**, **6b** and the two amide-/urea-functionalized derivatives **7b** and **9b**, were selected.

Figure 6, top, compares the influence of the type of hydrogen-bonding units in the head-group moiety (bisamide or amide/urea) on the sol–gel transition temperature (T_{gel}) in valeronitrile. It was found, similar to the *p*-xylene gels (Figure 2, top), that the sol–gel transition temperatures with the amide/urea compound **9b** are higher than with the bisamide **5b**. In both cases, the T_{gel} values of the valeronitrile gels are lower than the corresponding *p*-xylene gels. For example, at a concentration of 1.0 wt% compound **5b** reveals a T_{gel} of 90°C in *p*-xylene, but of 64°C in valeronitrile.

The influence on the T_{gel} of a kink in the head-group moiety was investigated by using the rigid derivative **5b** and the kinked derivative **6b**. As shown in Figure 6, middle, the same trend as in *p*-xylene gels was observed for the valeronitrile gel. Here too, the sol–gel transition temperatures are lower. The rigid derivative **5b** causes lower T_{gel} values of valeronitrile gels than does the kinked derivative **6b**. The same was observed in *p*-xylene gels (Figure 2, middle). Notably, compound **5b** had a broad gel-formation range (0.5 to 3.0 wt%), whereas compound **6b** forms gels at concentrations of between 2.0 and 3.0 wt%.

The results of introducing the lateral methyl substituent are shown in Figure 6, bottom, and are discussed for the solvent 3-methoxypropionitrile, whereby the same tendency was also found with valeronitrile. The amide-/urea-functionalized derivative **9b** with a lateral methyl substituent and the derivative **7b** without a methyl substituent were selected. The T_{gel} values of 3-methoxypropionitrile over the entire concentration range are about 10°C higher for compound **9b** with the methyl substituent than for compound **7b**. The same behavior was observed in *p*-xylene gels (Figure 2, bottom).

In conclusion, this comparison demonstrates that for both solvent systems, the nonpolar *p*-xylene and the polar solvents (valeronitrile and 3-methoxypropionitrile), the same underlying self-assembly principle is present and the difference depends mainly on the solubility of the organogelator.

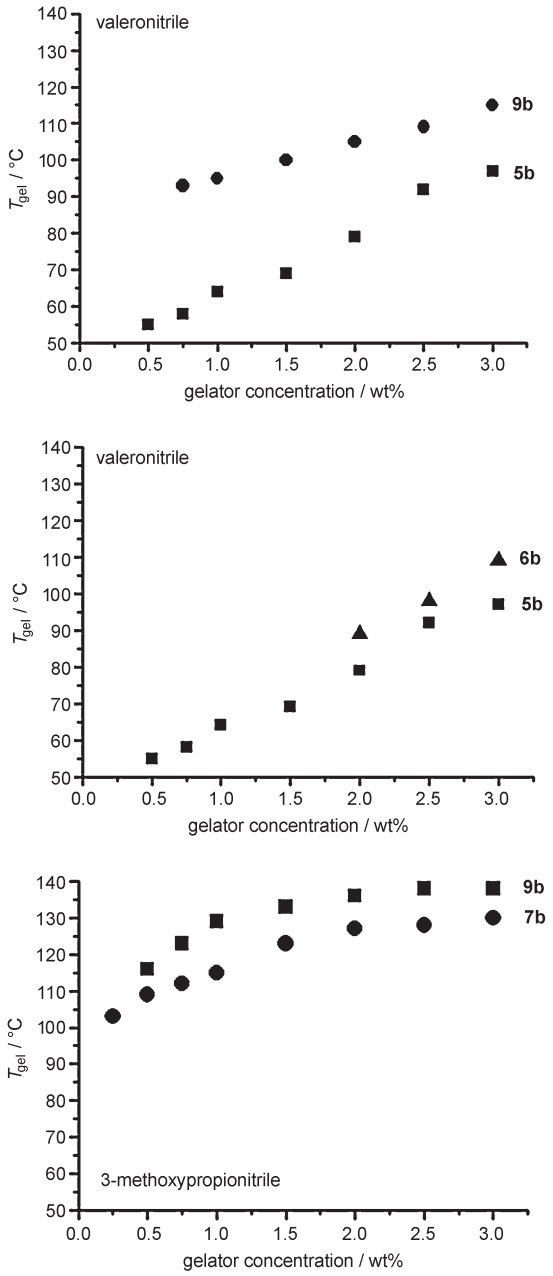

Figure 6. Sol–gel transition temperature as a function of the gelator concentration of several compounds in valeronitrile and 3-methoxypropionitrile. The influence of the different structural variations of the compounds is illustrated. Top: comparison of hydrogen-bonding units (amide or urea); middle: comparison of the position at the aromatic ring (*para* or *meta*); bottom: comparison of the substitution in the 2-position (with or without methyl group).

Conclusion

To date, prediction of gelation capability and efficiency has been nearly impossible. As reported in comparable studies, for example, those of Feringa and co-workers,[8,30] basic structure–property relationships with new molecules have to be established in order to optimize and tailor organogelators. Common to all these studies is a careful balance of molecular symmetry/asymmetry, hydrogen-bonding moieties, and units that provide the necessary solubility.

The present study of a particular set of amphiphilic asymmetrical molecules and experiments revealed that within this class of organogelators, the gelation capability, that is, the sol–gel transition temperature at low concentrations, and the optical properties of the resulting gels are improved by introducing a lateral methyl group at the hydrogen-bonding moiety. This improvement is visible in rigid *para*-linked as well as in kinked *meta*-linked head-groups. This phenomenon may be more general and transferable to the symmetrically designed organogelators.

The structure–property relationships established and described here can also be utilized to accelerate the discovery of efficient gelators for other solvents, for example, highly viscous materials or ionic liquids, with different solubility behavior, that is, polarity and boiling point.

In summary, this work is a further step towards establishing general structure–property relationships and supports a universally valid understanding of the gelation phenomenon.

Experimental Section

Materials and methods: Solvents for synthesis were purified and dried as necessary according to standard procedures. The amines and isocyanates used were obtained from Aldrich and Fluka and were used as received. Solvents for gelation tests were obtained from Merck–Suchardt and Fluka and were used as received. ^{1}H NMR spectra were recorded at room temperature by using a Bruker AC 250 instrument. Mass spectra were recorded by using the Mass Spectrometer VARIAN MAT CH-7 instrument (direct probe inlet, electron impact ionization) at the Central Analytic Laboratories of the University of Bayreuth. Elemental analysis was carried out by using an EA 3000 instrument (HEKAtech) at the Department of Chemical Engineering (Prof. A. Jess) of the University of Bayreuth.

General synthetic route to substituted aminophenyl amides 2a—d: The different amines (**1a–d**) (0.1 mol) were dissolved in dry *N*-methyl-2-pyrrolidone (150 mL) and dry pyridine (20 mL), and approximately 0.05 g of dried LiCl was added. The cyclohexanecarboxylic acid chloride (0.1 mol) was added and the mixture was stirred for 2 h at 80 °C. After cooling to room temperature, the mixture was precipitated in ice water (500 mL). The mixture was filtered (glass filter G3) to retrieve the solid, which was washed with water and dried. The resulting products were purified by recrystallization from methanol. Yields after recrystallization varied from 70 to 90 %. The obtained nitro compounds were dissolved in a mixture of THF (200 mL) and methanol (40 mL), to which Pd/C (1 g; 10 wt % Pd on activated carbon) was added. This mixture was stirred in an autoclave for 24 h at 40 °C with H_2 pressure of 3.5 bar. The colorless mixture was filtered (Alox N) and the solvents were evaporated. Subsequently, the obtained solid was purified by performing column chromatography on silica gel (1:1 hexane/EtOAc) to yield the white amino compounds **2a–d**. The ^{1}H NMR data of the individual compounds are given below.

Cyclohexanecarboxylic acid(4-aminophenyl)amide (2a): ^{1}H NMR ([D$_6$]DMSO, 250 MHz): $\delta = 1.51$ (m, 10H), 2.24 (m, 1H), 4.75 (s, 2H), 5.83 (s, 1H), 6.67 (d, $J = 8.7$ Hz, 2H), 7.05 ppm (m, $J = 8.7$ Hz, 2H).

Cyclohexanecarboxylic acid(3-aminophenyl)amide (2b): ^{1}H NMR ([D$_6$]DMSO, 250 MHz): $\delta = 1.31$ (m, 5H), 1.71 (m, 5H), 2.27 (s, 1H), 4.97 (s, 2H), 6.20 (d, $J = 8.8$ Hz, 1H), 6.66 (m, $J = 8.8$ Hz, 1H), 6.88 (m, 2H), 9.43 ppm (s, 1H).

Cyclohexanecarboxylic acid[4-amino(2-methyl)phenyl]amide (2c): ^{1}H NMR ([D$_6$]DMSO, 250 MHz): $\delta = 1.44$ (m, 10H), 1.98 (s, 3H), 2.26 (s,

1H), 4.85 (s, 2H), 6.33 (m, 2H), 6.79 (d, $J=8.2$ Hz, 1H), 8.79 ppm (s, 1H).

Cyclohexanecarboxylic acid[3-amino(2-methyl)phenyl]amide (2d): ^{1}H NMR ([D$_6$]DMSO, 250 MHz): $\delta=1.47$ (m, 10H), 1.85 (s, 3H), 2.33 (s, 1H), 4.79 (s, 2H), 6.45 (m, 2H), 6.80 (m, $J=8.2$ Hz, 1H), 9.03 ppm (s, 1H).

The syntheses of compounds **3a–c** are described in our previous work.[34]

Cyclohexanecarboxylic acid(3-octoylaminophenyl)amide (4a): The amino compound **2b** (1.2 g, 6.0 mmol) was dissolved in 50 mL NMP and dry pyridine (15 mL), and approximately 0.05 g of dried LiCl was added. The octoyl chloride (1.2 mL, 7 mmol) was added and the mixture was stirred for 2 h at 80 °C. After cooling to room temperature, the mixture was precipitated in ice water (1000 mL). The mixture was filtered (glass filter G3) to retrieve the solid, which was washed with water and dried. The crude product was suspended in boiling hexane, and THF was added dropwise to obtain a clear solution. For crystallization, the solution was stored at 4 °C for 12 h to retrieve a white solid. Yield 0.91 g of a white powder (44%, 2.6 mmol): m.p. 127 °C; $R_f=0.34$ (1:1 hexane/THF); ^{1}H NMR ([D$_6$]DMSO, 250 MHz): $\delta=0.86$ (t, $J=7.0$ Hz, 3H), 1.26 (m, 15H), 1.57 (m, 3H), 1.76 (m, 4H), 2.27 (m, 3H), 7.22 (m, 3H), 7.92 (s, 1H), 9.76 (s, 1H), 9.80 ppm (s, 1H); MS: m/z (%): 344 (24) [M^+]; elemental analysis calcd (%) for $C_{21}H_{32}N_2O_2$ (344.25): C 73.22, H 9.36, N 8.13; found: C 73.28, H 9.31, N 8.11.

Cyclohexanecarboxylic acid(3-tetradecoylaminophenyl)amide (4b): This compound was prepared as described for **4a**, starting from amino compound **2b** (1.2 g, 6.0 mmol) and tetradecoyl chloride (1.97 mL, 7 mmol). The product was purified by recrystallization from methanol/water 10:1. Yield 1.55 g of a white powder (60%, 3.6 mmol): m.p. 134 °C; $R_f=0.36$ (1:1 hexane/THF); ^{1}H NMR ([D$_6$]DMSO, 250 MHz): $\delta=0.85$ (t, $J=7.1$ Hz, 3H), 1.23 (m, 25H), 1.56 (m, 3H), 1.76 (m, 4H), 2.27 (m, 3H), 7.20 (m, 3H), 7.92 (s, 1H), 9.76 (s, 1H), 9.80 ppm (s, 1H); MS: m/z (%): 428 (39) [M^+]; elemental analysis calcd (%) for $C_{27}H_{44}N_2O_2$ (428.34): C 75.65, H 10.35, N 6.54; found: C 76.38, H 10.31, N 6.45.

Cyclohexanecarboxylic acid(3-octadecoylaminophenyl)amide (4c): This compound was prepared as described for **4a**, starting from amino compound **2b** (1.09 g, 5.0 mmol) and octadecoyl chloride (1.82 g, 6 mmol). The product was purified by recrystallization from methanol/water 10:1. Yield 1.8 g of a white powder (74%, 3.7 mmol): m.p. 116 °C; $R_f=0.38$ (1:1 hexane/THF); ^{1}H NMR ([D$_6$]DMSO, 250 MHz): $\delta=0.85$ (t, $J=7.1$ Hz, 3H), 1.23 (m, 33H), 1.57 (m, 3H), 1.76 (m, 4H), 2.27 (m, 3H), 7.19 (m, 3H), 7.92 (s, 1H), 9.76 (s, 1H), 9.80 ppm (s, 1H); MS: m/z (%): 484 (48) [M^+]; elemental analysis calcd (%) for $C_{31}H_{52}N_2O_2$ (484.4): C 76.81, H 10.81, N 5.78; found: C 76.88, H 10.91, N 5.71.

Cyclohexanecarboxylic acid[4-octoylamino(2-methyl)phenyl]amide (5a): This compound was prepared as described for **4a**, starting from amino compound **2c** (1.16 g, 5.0 mmol) and octoyl chloride (1.03 mL, 6 mmol). The product was purified by recrystallization from acetone. Yield 1.38 g of a white powder (77%, 3.8 mmol): m.p. 200 °C; $R_f=0.60$ (1:1 hexane/THF); ^{1}H NMR ([D$_6$]DMSO, 250 MHz): $\delta=0.85$ (t, $J=7.1$ Hz, 3H), 1.26 (m, 15H), 1.58 (m, 2H), 1.77 (m, 2H), 2.10 (s, 3H), 2.25 (t, $J=7.3$ Hz, 2H), 2.35 (m, 1H), 7.15 (d, $J=8.7$ Hz, 1H), 7.30 (d, $J=8.7$ Hz, 1H), 7.41 (s, 1H), 9.04 (s, 1H), 9.73 ppm (s, 1H); MS: m/z (%): 358 (43) [M^+]; elemental analysis calcd (%) for $C_{22}H_{34}N_2O_2$ (358.52): C 73.70, H 9.56, N 7.81; found: C 73.63, H 9.66, N 7.85.

Cyclohexanecarboxylic acid[4-tetradecoylamino(2-methyl)phenyl]amide (5b): This compound was prepared as described for **4a**, starting from amino compound **2c** (1.16 g, 5.0 mmol) and tetradecoyl chloride (1.63 mL, 6 mmol). The product was purified by recrystallization from acetone. Yield 1.47 g of a white powder (66%, 3.3 mmol): m.p. 188 °C; $R_f=0.62$ (1:1 hexane/THF); ^{1}H NMR (5:1 CDCl$_3$/CF$_3$COOD, 250 MHz): $\delta=0.87$ (t, $J=7.0$ Hz, 3H), 1.28 (m, 24H), 1.76 (m, 3H), 1.89 (m, 2H), 2.07 (m, 2H), 2.23 (s, 3H), 2.29 (m, 1H), 2.55 (t, $J=7.6$ Hz, 2H), 7.29 ppm (m, 3H); MS: m/z (%): 442 (100) [M^+]; elemental analysis calcd (%) for $C_{28}H_{46}N_2O_2$ (442.68): C 75.97, H 10.47, N 6.33; found: C 75.85, H 10.56, N 6.41.

Cyclohexanecarboxylic acid[4-octadecoylamino(2-methyl)phenyl]amide (5c): This compound was prepared as described for **4a**, starting from amino compound **2c** (1.16 g, 5.0 mmol) and octadecoyl chloride (1.82 g, 6 mmol). The product was purified by recrystallization from acetone. Yield 1.46 g of a white powder (58%, 2.9 mmol): m.p. 185 °C; $R_f=0.64$ (1:1 hexane/THF); ^{1}H NMR (5:1 CDCl$_3$/CF$_3$COOD, 250 MHz): $\delta=0.87$ (t, $J=7.0$ Hz, 3H), 1.25 (m, 32H), 1.76 (m, 3H), 1.91 (m, 2H), 2.07 (m, 2H), 2.23 (s, 3H), 2.29 (m, 1H), 2.54 (t, $J=7.6$ Hz, 2H), 7.29 ppm (m, 3H); MS: m/z (%): 498 (52) [M^+]; elemental analysis calcd (%) for $C_{32}H_{54}N_2O_2$ (498.79): C 77.06, H 10.91, N 5.62; found: C 76.46, H 10.86, N 5.68.

Cyclohexanecarboxylic acid[3-octoylamino(2-methyl)phenyl]amide (6a): This compound was prepared as described for **4a**, starting from amino compound **2d** (1.16 g, 5.0 mmol) and octoyl chloride (1.03 mL, 6 mmol). The product was purified by recrystallization from THF. Yield 1.30 g of a white powder (73%, 3.6 mmol): m.p. 210 °C; $R_f=0.50$ (1:1 hexane/THF); ^{1}H NMR ([D$_6$]DMSO, 250 MHz): $\delta=0.86$ (t, $J=7.0$ Hz, 3H), 1.28 (m, 15H), 1.58 (m, 2H), 1.78 (m, 2H), 1.98 (s, 3H), 2.29 (m, 3H), 7.09 (s, 3H), 9.19 (s, 1H), 9.28 ppm (s, 1H); MS: m/z (%): 358 (64) [M^+]; elemental analysis calcd (%) for $C_{22}H_{34}N_2O_2$ (358.52): C 73.70, H 9.56, N 7.81; found: C 73.82, H 9.69, N 7.73.

Cyclohexanecarboxylic acid[3-tetradecoylamino(2-methyl)phenyl]amide (6b): This compound was prepared as described for **4a**, starting from amino compound **2d** (1.16 g, 5.0 mmol) and tetradecoyl chloride (1.63 mL, 6 mmol). The product was purified by recrystallization from THF. Yield 1.96 g of a white powder (86%, 4.4 mmol): m.p. 202 °C; $R_f=0.54$ (1:1 hexane/THF); ^{1}H NMR (5:1 CDCl$_3$/CF$_3$COOD, 250 MHz): $\delta=0.87$ (t, $J=7.0$ Hz, 3H), 1.28 (m, 27H), 1.81 (m, 2H), 1.90 (m, 2H), 2.10 (m, 4H), 2.63 (m, 2H), 7.27 ppm (m, 3H); MS: m/z (%): 442 (78) [M^+]; elemental analysis calcd (%) for $C_{28}H_{46}N_2O_2$ (442.68): C 75.97, H 10.47, N 6.33; found: C 75.70, H 10.63, N 6.31.

Cyclohexanecarboxylic acid[3-octadecoylamino(2-methyl)phenyl]amide (6c): This compound was prepared as described for **4a**, starting from amino compound **2d** (1.16 g, 5.0 mmol) and octadecoyl chloride (1.82 g, 6 mmol). The product was purified by recrystallization from DMF. Yield 1.84 g of a white powder (74%, 3.7 mmol): m.p. 199 °C; $R_f=0.58$ (1:1 hexane/THF); ^{1}H NMR (5:1 CDCl$_3$/CF$_3$COOD, 250 MHz): $\delta=0.87$ (t, $J=6.8$ Hz, 3H), 1.28 (m, 35H), 1.81 (m, 2H), 1.92 (m, 2H), 2.12 (m, 4H), 2.63 (m, 2H), 7.27 ppm (m, 3H); MS: m/z (%): 498 (91) [M^+]; elemental analysis calcd (%) for $C_{32}H_{54}N_2O_2$ (498.79): C 77.06, H 10.91, N 5.62; found: C 77.05, H 11.07, N 5.73.

The syntheses of compounds **7a–c** are described in our previous work.[34]

Cyclohexanecarboxylic acid[3-(3-octylureido)phenyl]amide (8a): A solution of amino compound **2b** (1.07 g, 5.0 mmol) in THF (50 mL) was added to a solution of octylisocyanate (0.93 mL, 6.0 mmol) in THF (15 mL). The reaction mixture was refluxed for 2 h. After cooling to room temperature, the mixture was added to methanol (80 mL) and evaporated to the halfway point. The precipitation began while cooling to room temperature. After 2 h, the mixture was filtered (glass filter G3) to retrieve the solid, which was washed with water and dried. The product was purified by recrystallization from methanol. Yield 1.56 g of a white powder (84%, 4.2 mmol); m.p. 159 °C; $R_f=0.52$ (1:1 hexane/THF); ^{1}H NMR (5:1 CDCl$_3$/CF$_3$COOD, 250 MHz): $\delta=0.89$ (t, $J=7.0$ Hz, 3H), 1.46 (m, 17H), 1.91 (m, 5H), 2.44 (m, 1H), 3.35 (t, $J=7.4$ Hz, 2H), 7.16 (m, 1H), 7.42 ppm (m, 3H); MS: m/z (%): 373 (28) [M^+]; elemental analysis calcd (%) for $C_{22}H_{35}N_3O_2$ (373.54): C 70.74, H 9.44, N 11.25; found: C 70.43, H 9.58, N 11.26.

Cyclohexanecarboxylic acid[3-(3-tetradecylureido)phenyl]amide (8b): This compound was prepared as described for **8a**, starting from amino compound **2b** (1.09 g, 5.0 mmol) and tetradecylisocyanate (1.44 g, 6.0 mmol). The product was purified by recrystallization from methanol. Yield 1.55 g of a white powder (68%, 3.4 mmol); m.p. 146 °C; $R_f=0.58$ (1:1 hexane/THF); ^{1}H NMR (5:1 CDCl$_3$/CF$_3$COOD, 250 MHz): $\delta=0.87$ (t, $J=7.0$ Hz, 3H), 1.39 (m, 29H), 1.90 (m, 5H), 2.45 (m, 1H), 3.35 (t, $J=7.3$ Hz, 2H), 7.17 (m, 1H), 7.42 ppm (m, 3H); MS: m/z (%): 457 (8) [M^+]; elemental analysis calcd (%) for $C_{28}H_{47}N_3O_2$ (457.71): C 73.48, H 10.35, N 9.18; found: C 72.99, H 10.67, N 8.72.

Cyclohexanecarboxylic acid[3-(3-octadecylureido)phenyl]amide (8c): This compound was prepared as described for **8a**, starting from amino compound **2b** (1.09 g, 5.0 mmol) and octadecylisocyanate (1.77 g,

6.0 mmol). The product was purified by recrystallization from THF. Yield 2.33 g of a white powder (91%, 4.5 mmol); m.p. 142°C; R_f=0.64 (1:1 hexane/THF); ^{1}H NMR (5:1 $CDCl_3$/CF_3COOD, 250 MHz): δ=0.87 (t, J=7.0 Hz, 3H), 1.48 (m, 37H), 1.90 (m, 5H), 2.45 (m, 1H), 3.35 (t, J=7.3 Hz, 2H), 7.17 (m, 1H), 7.44 ppm (m, 3H); MS: m/z (%): 513 (13) [M^+]; elemental analysis calcd (%) for $C_{32}H_{55}N_3O_2$ (513.81): C 74.80, H 10.79, N 8.18; found: C 74.59, H 11.20, N 7.62.

Cyclohexanecarboxylic acid[2-methyl-4-(3-octylureido)phenyl]amide (9a): This compound was prepared as described for **8a**, starting from amino compound **2c** (1.16 g, 5.0 mmol) and octylisocyanate (0.93 g, 6.0 mmol). The product was purified by recrystallization from DMF. Yield 1.29 g of a white powder (67%, 3.3 mmol); m.p. 231°C (decomp) ; R_f=0.32 (1:1 hexane/THF); ^{1}H NMR (5:1 $CDCl_3$/CF_3COOD, 250 MHz): δ=0.86 (t, J=7.0 Hz, 3H), 1.42 (m, 17H), 1.92 (m, 5H), 2.25 (s, 3H), 2.54 (m, 1H), 3.35 (t, J=7.1 Hz, 2H), 7.14 (m, 2H), 7.40 ppm (d, J=8.4 Hz, 1H); MS: m/z (%): 387 (46) [M^+]; elemental analysis calcd (%) for $C_{23}H_{37}N_3O_2$ (387.57): C 71.28, H 9.62, N 10.84; found: C 71.61, H 9.71, N 10.79.

Cyclohexanecarboxylic acid[2-methyl-4-(3-tetradecylureido)phenyl]-amide (9b): This compound was prepared as described for **8a**, starting from amino compound **2c** (1.16 g, 5.0 mmol) and tetradecylisocyanate (1.44 g, 6.0 mmol). The product was purified by recrystallization from DMF. Yield 1.86 g of a white powder (78%, 3.9 mmol); m.p. 227°C (decomp) ; R_f=0.38 (1:1 hexane/THF); ^{1}H NMR (5:1 $CDCl_3$/CF_3COOD, 250 MHz): δ=0.87 (t, J=7.0 Hz, 3H), 1.49 (m, 29H), 1.92 (m, 5H), 2.25 (s, 3H), 2.52 (m, 1H), 3.35 (t, J=7.3 Hz, 2H), 7.16 (m, 2H), 7.40 ppm (d, J=8.4 Hz, 1H); MS: m/z (%): 471 (86) [M^+]; elemental analysis calcd (%) for $C_{29}H_{49}N_3O_2$ (471.73): C 73.84, H 10.47, N 8.91; found: C 73.54, H 10.56, N 8.91.

Cyclohexanecarboxylic acid[2-methyl-4-(3-octadecylureido)phenyl]amide (9c): This compound was prepared as described for **8a**, starting from amino compound **2c** (1.16 g, 5.0 mmol) and octadecylisocyanate (1.77 g, 6.0 mmol). The product was purified by recrystallization from DMF. Yield 2.13 g of a white powder (81%, 4.0 mmol); m.p. 228°C (decomp) ; R_f=0.44 (1:1 hexane/THF); ^{1}H NMR (5:1 $CDCl_3$/CF_3COOD, 250 MHz): δ=0.87 (t, J=7.0 Hz, 3H), 1.46 (m, 37H), 1.93 (m, 5H), 2.25 (s, 3H), 2.52 (m, 1H), 3.35 (t, J=7.6 Hz, 2H), 7.15 (m, 2H), 7.40 ppm (d, J=8.4 Hz, 1H); MS: m/z (%): 527 (13) [M^+]; elemental analysis calcd (%) for $C_{33}H_{57}N_3O_2$ (527.84): C 75.09, H 10.88, N 7.96; found: C 75.06, H 10.97, N 7.87.

Cyclohexanecarboxylic acid[2-methyl-3-(3-octylureido)phenyl]amide (10a): This compound was prepared as described for **8a**, starting from amino compound **2d** (1.16 g, 5.0 mmol) and octylisocyanate (0.93 g, 6.0 mmol). The product was purified by recrystallization from DMF. Yield 1.35 g of a white powder (70%, 3.4 mmol); m.p. 246°C (decomp) ; R_f=0.46 (1:1 hexane/THF); ^{1}H NMR (5:1 $CDCl_3$/CF_3COOD, 250 MHz): δ=0.78 (t, J=7.0 Hz, 3H), 1.41 (m, 17H), 1.85 (m, 5H), 2.10 (s, 3H), 2.47 (m, 1H), 3.26 (t, J=7.3 Hz, 2H), 7.22 ppm (m, 3H); MS: m/z (%): 387 (42) [M^+]; elemental analysis calcd (%) for $C_{23}H_{37}N_3O_2$ (387.57): C 71.28, H 9.62, N 10.84; found: C 70.97, H 9.65, N 10.87.

Cyclohexanecarboxylic acid[2-methyl-3-(3-tetradecylureido)phenyl]-amide (10b): This compound was prepared as described for **8a**, starting from amino compound **2d** (1.16 g, 5.0 mmol) and tetradecylisocyanate (1.44 g, 6.0 mmol). The product was purified by recrystallization from DMF. Yield 1.73 g of a white powder (73%, 3.7 mmol); m.p. 240°C (decomp) ; R_f=0.51 (1:1 hexane/THF); ^{1}H NMR (5:1 $CDCl_3$/CF_3COOD, 250 MHz): δ=0.87 (t, J=7.0 Hz, 3H), 1.47 (m, 29H), 1.92 (m, 5H), 2.19 (s, 3H), 2.53 (m, 1H), 3.34 (t, J=7.3 Hz, 2H), 7.29 ppm (m, 3H); MS: m/z (%): 471 (17) [M^+]; elemental analysis calcd (%) for $C_{29}H_{49}N_3O_2$ (471.73): C 73.84, H 10.47, N 8.91; found: C 73.77, H 10.47, N 8.93.

Cyclohexanecarboxylic acid[2-methyl-3-(3-octadecylureido)phenyl]amide (10c): This compound was prepared as described for **8a**, starting from amino compound **2d** (1.16 g, 5.0 mmol) and octadecylisocyanate (1.77 g, 6.0 mmol). The product was purified by recrystallization from DMF. Yield 2.05 g of a white powder (78%, 3.9 mmol); m.p. 233°C (decomp) ; R_f=0.56 (1:1 hexane/THF); ^{1}H NMR (5:1 $CDCl_3$/CF_3COOD, 250 MHz): δ=0.87 (t, J=7.0 Hz, 3H), 1.48 (m, 37H), 1.92 (m, 5H), 2.19 (s, 3H), 2.55 (m, 1H), 3.34 (t, J=7.3 Hz, 2H), 7.29 ppm (m, 3H); MS: m/z (%): 527 (18) [M^+]; elemental analysis calcd (%) for $C_{33}H_{57}N_3O_2$ (527.84): C 75.09, H 10.88, N 7.96; found: C 75.05, H 11.07, N 8.01.

Gelation tests: In a typical gelation test, a weighed amount of the compound was mixed with 2 mL of solvent in a test tube with a screw cap, and then the mixture was heated until the solid was completely dissolved. The resulting solution was allowed to cool slowly to room temperature. Gelation was considered to have occurred when a homogenous substance that exhibited no gravitational flow was obtained. For the determination of the sol–gel transition temperature (T_{gel}) of the gels, the steel-ball method was used.[30] A steel ball (260 mg) with a diameter of 4.5 mm was placed on top of the gel and the vial was sealed. The samples were placed in a heating system that was slowly heated, typically at 5°C min^{-1}, and the temperature was determined by using a temperature sensor that was dipped in a separate vial containing solvent. The T_{gel} of the gel was defined as the temperature at which the steel ball hit the bottom of the vial.

Electron microscopy: For TEM, a formar/carbon-coated copper grid (300 mesh) was dipped for a very short time (<1 s) in the solution of the gelator in the organic solvent and then laid on a weighing paper to become a gel. After 1 h, the grid was placed in a round-bottomed flask and dried at low pressure (<10^{-2} mbar). The grids were examined under a Zeiss CEM 902 electron microscope, operating at 80 kV. For SEM, a xerogel was prepared. Gels (2 mL) of a mixture of 1.0 wt% in *p*-xylene were prepared in a glass with a diameter of 22 mm. After 24 h at room temperature, the glass was placed in an autoclave (volume: 1 L; PARR Instrument Co., Frankfurt am Main). The autoclave was annealed at 8°C with a pressure of 56 bar. After an extraction time of 4 h, the CO_2 content was reduced to 10%. This process was repeated twice to ensure the complete extraction of *p*-xylene. The autoclave was refilled with CO_2 and after 2 h, the temperature was increased stepwise (2°C/10 min) up to 35°C to reach a pressure of 130 bar: the parameters of the supercritical CO_2. After 10 min, the pressure was reduced to 1 bar over 1 h. The SEM measurements were performed by using a LEO 1530 (FE-REM with Schottky-field-emision cathode) and an in-lens detector.

Optical properties: The standard optical characteristic "haze" was measured for the *p*-xylene gels by using a "Haze-Gard Plus" instrument (BYK Gardner GmbH, Germany), which conforms to ASTM D-1003. A homogeneous solution of the gelator in *p*-xylene at the different concentrations was poured into a quartz cell of volume 2 mL, diameter 18 mm, and thickness 10 mm. After cooling to room temperature at a cooling rate of 5°C min^{-1}, the gel was maintained at 25°C for 24 h before performing the measurement.

IR spectroscopy: The infrared measurements were performed by using a BIO-RAD Digilab FTS-40 spectrometer with a NaCl cell of diameter 2 mm. The gelator was dissolved in the *p*-xylene at elevated temperatures and then poured into the cell with a syringe through a closable opening. After cooling to room temperature at a cooling rate of 5°C min^{-1}, the gel was maintained at 25°C for 24 h before performing the measurement.

Acknowledgements

We thank N. Glaser and C. Abetz (BIMF) for the electron microscopy experiments and B. Brunner (Department of Chemical Engineering, Prof. A. Jess, University of Bayreuth) for performing the elemental analysis. We are also indebted to Sandra Ganzleben for her assistance in the synthesis of several compounds.

[1] P. Terech, R. G. Weiss, *Chem. Rev.* **1997**, *97*, 3133–3159.
[2] D. J. Abdallah, R. G. Weiss, *Adv. Mater.* **2000**, *12*, 1237–1247.
[3] G. Haering, P. L. Luisi, *J. Phys. Chem.* **1986**, *90*, 5892–5895.
[4] J. Fricke, A. Emmerling, *Adv. Mater.* **1991**, *3*, 504–506.
[5] W. Kubo, K. Murakoshi, T. Kitamura, S. Yoshida, M. Haruki, K. Hanabusa, H. Shirai, Y. Wada, S. J. Yanagida, *J. Phys. Chem. B* **2001**, *105*, 12809–12815.

[6] J.-M. Lehn, *Supramolecular Chemistry: Concepts and Perspectives*, VCH, Weinheim, **1995**.
[7] R. J. Phillips, W. M. Deen, J. F. Brady, *J. Colloid Interface Sci.* **1990**, *139*, 363–373.
[8] J. van Esch, S. De Feyter, R. M. Kellogg, F. De Schyver, B. L. Feringa, *Chem. Eur. J.* **1997**, *3*, 1238–1243.
[9] K. Hanabusa, M. Yamada, M. Kimura, H. Shirai, *Chem. Mater.* **1999**, *11*, 649–655.
[10] R. H. C. Janssen, V. Stümpflen, C. W. M. Bastiaansen, D. J. Broer, T. A. Tervoort, P. Smith, *Jpn. J. Appl. Phys.* **2000**, *39*, 2721–2726.
[11] M. Lescanne, P. Grondin, A. d'Aléo, F. Fages, J. L. Pozzo, O. Mondain-Monval, P. Reinheimer, A. Colin, *Langmuir* **2004**, *20*, 3032–3041.
[12] K. J. C. van Bommel, C. van der Pol, I. Muizebelt, A. Friggeri, A. Heeres, A. Meetsma, B. L. Feringa, J. van Esch, *Angew. Chem.* **2004**, *116*, 1695–1699; *Angew. Chem. Int. Ed.* **2004**, *43*, 1663–1667.
[13] U. Beginn, B. Tartsch, *Chem. Commun.* **2001**, 1924–1925.
[14] R. P. Sijbesma, E. W. Meijer, *Chem. Commun.* **2003**, 5–16.
[15] S. Boileau, L. Bouteiller, F. Laupretre, F. Lortie, *New J. Chem.* **2000**, *24*, 845–848.
[16] F. Würthner, C. Thalacker, A. Sautter, *Adv. Mater.* **1999**, *11*, 754–758.
[17] S. Yamasaki, H. Tsutsumi, *Bull. Chem. Soc. Jpn.* **1994**, *67*, 906–911.
[18] J. M. Smith, D. E. Katsoulis, *J. Mater. Chem.* **1995**, *5*, 1899–1903.
[19] N. Mohmeyer, P. Wang, H.-W. Schmidt, S. M. Zakeeruddin, M. Grätzel, *J. Mater. Chem.* **2004**, *14*, 1905–1909.
[20] I. O. Shklyarevskiy, P. Jonkheijm, P. C. M. Christianen, A. P. H. J. Schenning, A. Del Guerzo, J.-P. Desvergne, E. W. Meijer, J. C. Maan, *Langmuir* **2005**, *21*, 2108–2112.
[21] F. Placin, J.-P. Desvergne, J.-C. Lassègues, *Chem. Mater.* **2001**, *13*, 117–121.
[22] Y.-C. Lin, R. G. Weiss, *Macromolecules* **1987**, *20*, 414–417.
[23] J. Nagasawa, M. Kudo, S. Hayashi, N. Tamaoki, *Langmuir* **2004**, *20*, 7907–7916.
[24] K. Sugiyasu, N. Fujita, S. Shinkai, *Angew. Chem.* **2004**, *116*, 1249–1253; *Angew. Chem. Int. Ed.* **2004**, *43*, 1229–1233.
[25] M. George, S. L. Snyder, P. Terech, C. J. Glinka, R. G. Weiss, *J. Am. Chem. Soc.* **2003**, *125*, 10275–10283.
[26] K. Hanabusa, R. Tanaka, M. Suzuki, M. Kimura, H. Shirai, *Adv. Mater.* **1997**, *9*, 1095–1097.
[27] K. Hanabusa, M. Yamada, M. Kimura, H. Shirai, *Angew. Chem.* **1996**, *108*, 2086–2088.
[28] M. George, G. Tan, V. T. John, R. G. Weiss, *Chem. Eur. J.* **2005**, *11*, 3243–3254.
[29] V. Simic, L. Bouteiller, M. Jalabert, *J. Am. Chem. Soc.* **2003**, *125*, 13148–13154.
[30] J. van Esch, F. Schoonbeek, M. de Loos, H. Kooijman, A. L. Spek, R. M. Kellogg, B. L. Feringa, *Chem. Eur. J.* **1999**, *5*, 937–950.
[31] O. Colombani, L. Bouteiller, *New J. Chem.* **2004**, *28*, 1373–1382.
[32] R. J. H. Hafkamp, M. C. Feiters, R. J. M. Nolte, *J. Org. Chem.* **1999**, *64*, 412–426.
[33] K. Yabuuchi, A. E. Rowan, R. J. M. Nolte, T. Kato, *Chem. Mater.* **2000**, *12*, 440–443.
[34] N. Mohmeyer, H.-W. Schmidt, *Chem. Eur. J.* **2005**, *11*, 863–872.
[35] W. Kubo, S. Kambe, S. Nakade, T. Kitamura, K. Hanabusa, Y. Wada, S. Yanagida, *J. Phys. Chem. B* **2003**, *107*, 4374–4381.
[36] W. Kubo, K. Murakoshi, T. Kitamura, *Chem. Lett.* **1998**, 1241–1242.
[37] E. Pretsch, T. Clerc, J. Seibl, W. Simon, *Structural Analysis of Organic Compounds*, Springer Verlag, Berlin, **1990**.
[38] F. S. Schoonbeek, J. van Esch, R. Hulst, R. M. Kellogg, B. L. Feringa, *Chem. Eur. J.* **2000**, *6*, 2633–2643.
[39] F. Lortie, S. Boileau, L. Bouteiller, *Chem. Eur. J.* **2003**, *9*, 3008–3014.
[40] ASTM Standard D 1003 Standard Test Method for Haze and Luminous Transmittance of Transparent Plastics, **1961**.

Received: August 9, 2006
Revised: January 3, 2007
Published online: March 9, 2007

